Colloid Polym Sci 276:160–168 (1998)

ORIGINAL CONTRIBUTION

C. Humbert
J.P. Decruppe

Stress optical coefficient of viscoelastic solutions of cetyltrimethylammonium bromide and potassium bromide

Received: 25 July 1997
Accepted: 10 October 1997

C. Humbert · J.P. Decruppe (✉)
Laboratoire de Physique des Liquides et interfaces
Groupe rhéophysique des Colloides
Université de Metz 1Bd.
D.F. Arago 57078 Metz
France
E-mail: Decruppe@lpli.univ-metz.fr

Abstract The rheo-optical properties of different viscoelastic solutions of surfactant are investigated in order to gather experimental data which allow for the computation of the stress optical coefficient C.

The surfactant which is the widely used cetyltrimethylammonium bromide (CTAB) is mixed with potassium bromide, in various amounts in order to vary the salinity of the solvent. Flow birefringence experiments and rheological measurements are performed on these solutions in order to study the dependence of the angle of extinction χ, of the birefringence intensity Δn and of the shear stress σ_{yx} with the shear rate $\dot{\gamma}$. These data are used to check the stress optical law which turns out to be valid in a wide range of shear rates. The stress optical coefficient C is then computed: it is found to vary with the concentration of surfactant and with the salinity of the solvent.

Key words Flow birefringence – shear flow – surfactant – stress optical rule

Introduction

Surfactant monomers are known to form very long micellar structures often called "worm-like" micelles under specific conditions of concentration and salinity of the solvent which usually is water containing some kind of salt or a co-surfactant. When the concentration is large enough, the long micelles will overlap forming entanglements which give interesting viscoelastic properties to the micellar solution. These solutions often show strong birefringence when subjected to the orientating action of shear flows, elongational flows, electric or magnetic fields. This is the case for the particular solution of cetyltrimethylammonium bromide (CTAB) in salted water which has already received much attention as confirmed by the number of papers published since the first experiments of Sheraga et al. [1, 2] and the works of Shikata et al. [3] or Wunderlich, Hoffmann and their collaborators [4, 5]. When subjected to the action of shearing forces in a Couette cell, these solutions show strong flow birefringence, the intensity of which is several times the values usually measured in semi-dilute solutions of polymers which makes it an ideal solution for the study of flow birefringence.

Rheological and optical data gathered from viscosity and birefringence measurements are related through the stress optical law which in the case of the different solutions studied in this work applies in a wide range of shear stresses. This law when it applies, states the proportionality of the stress tensor and the refractive index tensor and is expressed mathematically through two simple equations relating the optical characteristics of the medium, i.e. the angle of extinction χ and the birefringence intensity Δn to the components of the stress tensor; the proportionality coefficient is the so-called "stress optical coefficient" the study of which is the aim of this paper.

We report, in this work, on the rheo-optical behavior of different aqueous solutions of CTAB with various amounts of KBr subjected to a simple shear flow in a Couette cell for the optical measurements and in

a cone–plane device for the tangential shear stress measurements. These results allow for the computation of the stress optical coefficient C which in turn leads to the first normal stress difference N_1. The coefficient C is found to vary significantly with the concentration of both the components. This result is not in agreement with previous works on different micellar systems for which C is found to vary only little with the concentration of the surfactant or of the salt. It is the case for the system sodium lauryl polyoxyethylene sulfate with $NaNO_3$ of Janeschitz–Kriegl and Papenhuijzen [6] and for CTAB/NaSal of Shikata [3]. The temperature dependence of the coefficient is found to agree with the theoretical expression of C.

Theoretical section

The stress optical law was first derived by Lodge [7] and later extended to overlapping rod-like particles by Doi and Edwards [8]. This law relates in a simple way the refractive index tensor $\mathbf{n}$ and the stress tensor $\boldsymbol{\tau}$:

$$\mathbf{n} = C\boldsymbol{\tau} + A\mathbf{I} ,$$

where A is a constant, $\mathbf{I}$ the unit tensor and C the stress optical coefficient.

In a coordinate system the Ox axis of which is in the direction of the flow (Oz being perpendicular to the plane of the flow) this latter relation is expressed in terms of two simple equations:

$$\Delta n \sin(2\chi) = 2C\sigma_{yx} , \tag{1}$$

$$\Delta n \cos(2\chi) = CN_1 = C(\sigma_{xx} - \sigma_{yy}) , \tag{2}$$

where χ and Δn are the optical characteristics of the solution. χ stands for the angle of extinction and Δn for the birefringence intensity. The angle χ is defined as the acute angle between a neutral line and the direction of flow (Ox direction) and Δn is related to the retardance ϕ of the medium by the simple equation $\Delta n = \phi\lambda_0/2\pi e$.

In the case of a simple shear flow in the x direction between parallel plates, the only non-diagonal terms of the stress tensor which is non-zero is σ_{yx}. N_1 is the first normal stress difference. Measuring normal forces accurately is far from an easy task to do, but in the domain of validity of the stress optical law, N_1 can be computed from optical measurements which in the case of micellar solutions are rather easily performed. The stress optical rule only takes into account the intrinsic birefringence resulting from the polarizability anisotropy of the dissolved particles. When form birefringence which arises from the difference between the mean refractive index of a particle and the solvent is present, the stress optical law is no longer valid. Significant deviations from the law will be found in that case.

The simplest mathematical model used to describe a visocelastic solution is Maxwell's model. Under small harmonic oscillations, the dynamic characteristics of this model, G' the storage modulus and G'' the loss modulus, are simple functions of the angular frequency ω of the motion:

$$G'(\omega) = \frac{G_0\omega^2\tau^2}{1+\omega^2\tau^2} , \qquad G''(\omega) = \frac{G_0\omega\tau}{1+\omega^2\tau^2} . \tag{3}$$

The storage modulus G' measured as a function of ω is particularly interesting since it can be used to check the accuracy of the stress optical coefficient. The first normal stress difference N_1 is computed from Eq. (2) once the coefficient C has been found with the first equation. N_1 and G' should meet in Laun's relation [9–11].

$$\left(\frac{G'(\omega)}{\omega^2}\right)_{\omega\to 0} = \left(\frac{N_1}{2\dot\gamma^2}\right)_{\dot\gamma\to 0} = \left(\frac{\Delta n\cos(2\chi)}{2C\dot\gamma^2}\right)_{\dot\gamma\to 0} . \tag{4}$$

This simple equation relates G' which results from dynamical rheological measurements with the optical characteristics χ and Δn of the medium which are performed under permanent shear flows. It will also be of great use when checking the validity of our experimental measurements.

Experimental section

Materials

The surfactant used in this work is the well-known cetyltrimethylammonium bromide (CTAB) which is sold by Jansen Chemical. The chemical is used without any purification, mixed with a salt, KBr, in distilled water. The solution is kept at a temperature of 40 °C for a few days in order to reach equilibrium. Two sets of solutions have been studied: the first one consists of four aqueous solutions of equal ionic strength (0.1 M KBr) with an increasing amount of surfactant (0.3, 0.4, 0.5, 0.6 M) while, for the second, the concentration of CTAB is kept constant (0.3 M) and the proportion of salt (KBr) is gradually increased to give four solutions at 0.1, 0.2, 0.3 and 0.4 M.

Experimental devices

The measurements of the extinction angle χ and of the retardance ϕ are performed with a home-built polarimeter bench described with many details in an earlier paper [12]. It consists of the few elements necessary to measure χ and ϕ by the classical method of Senarmont: a pair of crossed

polarizers, a quarter-wave plate and a light beam (He–Ne laser). The solution is subjected to the shear flow in a stainless-steel Couette cell. Various dimensions of the cell have been used to check the accuracy of our measurements. Three different optical lengths of the cell have been used to study the importance of the ends effects on the measurements. The diameter of the inner cylinder is 47 mm giving a gap of 1.5 mm. Two different devices have been used to perform the rheological experiments: a rheometer (Carrimed CLS 100) using a cone–plane device working in constant shear mode and a Haake PK 100 using a Couette device but working in constant shear rate mode. The measurements performed with both apparatus are in very good agreement and no significant discrepancy can be found in the results. The temperature is kept constant within 0.025 °C and all measurements were performed at 30 °C except for the equimolar solution ($C_D = C_S =$ 0.3 M) the temperature of which takes five values between 30 °C and 38 °C.

Experimental results

Optical results and curves

Three different sets of results shall now be presented and discussed in the following. The first one (set I) refers to the single equimolar solution (0.3 M in CTAB and KBr) studied at different temperatures chosen between 30 °C and 38 °C. The second set (set II) concerns the result of four solutions containing the same amount of surfactant in a solvent. In the last set (set III), the salinity of the solvent is kept constant (0.1 M in KBr) while the concentration in surfactant changes from 0.3 to 0.6 M. The solution CTAB/KBr 0.3/0.1 M is also the test solution for the study of the ends effects.

Performing an experiment of birefringence consists in measuring two optical quantities acquired by the solution subjected to a shear flow χ and ϕ. In a laboratory frame one axis of which is in the direction of flow, χ is the acute angle between this axis and one arm of the cross of isocline, while ϕ is the retardance of the medium.

As already quoted, Couette cells of various optical lengths have been used in order to perform these measurements. The length of the cell is chosen according to the value of the retardance ϕ which can easily reach 2π with solutions of surfactants. Solutions having a high concentration of surfactant ($C_D = 0.6$ M) or a high concentration in salt ($C_S = 0.4$ M for example) when C_D is small ($C_D = 0.1$ M) show strong birefringence which we shall easily and accurately characterize with a 30 mm optical path cell. However, the smaller the optical path the more important the ends effects near the closing windows. These ends effects cause a decrease of the retardance ϕ and make the determination of χ inaccurate. As a matter of fact, the small volume of liquid disturbed near the end windows, acts as a depolarizing device on the incident light beam and in the process of measuring χ and ϕ, the extinction cannot be achieved perfectly. Figure 1 shows the behavior of ϕ and Δn versus $\dot{\gamma}$ at 30 °C for different heights ($h = 30$, 50 and 73 mm) for a solution of CTAB with KBr ($C_D = 0.3$ M, $C_S = 0.1$ M) subjected to shear rates $\dot{\gamma}$ up to 180 s^{-1}. The agreement between the curves is found over the entire range of $\dot{\gamma}$ with a fairly good approximation, showing thus that the ends effects are of little importance with these highly birefringent solutions.

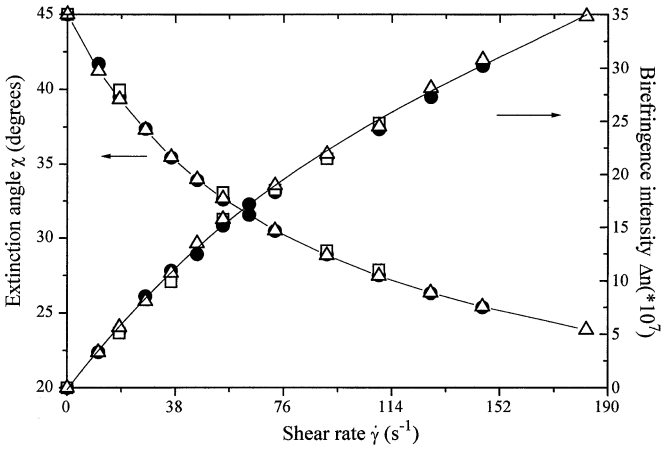

Fig. 1 Extinction angle χ and birefringence intensity Δn versus shear rate $\dot{\gamma}$ for various optical path lengths; the symbols respectively, correspond, to a length of: (△) 30 mm, (□) 50 mm and (●) 73 mm

Set I: Equimolar solution of CTAB and KBr ($C_D = C_S = 0.3$ M)

The next curves (see Figs. 2a and b) show the variations of χ and Δn (absolute value of Δn) as a function of $\dot{\gamma}$ for five different temperatures in the case of the equimolar solution ($C_D = C_S = 0.3$ M). The birefringence intensity has been found to be negative for all solutions studied in this work.

The overall behavior of these two quantities is consistent with what is usually observed. $\chi(\dot{\gamma})$ decreases at first while $\Delta n(\dot{\gamma})$ at the same time increases as a result of a better orientation of the micelles in the flow. The slope of the first part decreases with T in the curves $\Delta n(\dot{\gamma})$ while the absolute value of the slope increases with T in the curve $\chi(\dot{\gamma})$. This behavior is consistent with the fact that the average length of the particles diminishes with T and the influence of the Brownian motion, which tends to disorganize the particles, is thus strengthened. If $\dot{\gamma}$ is further increased, χ or

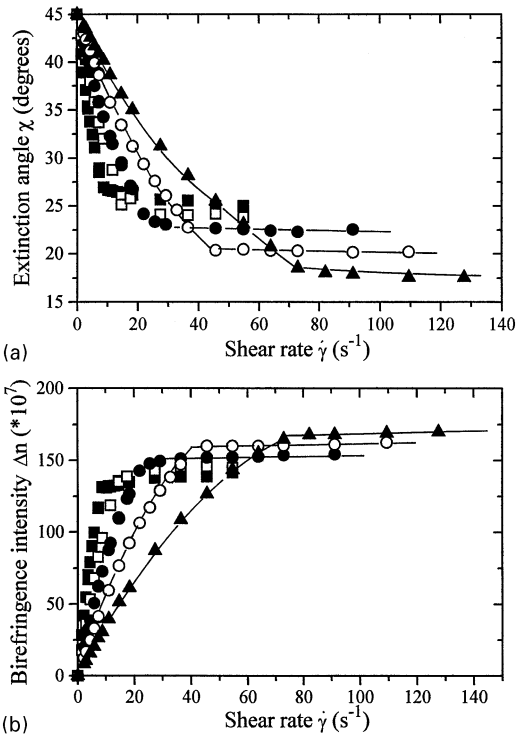

Fig. 2a, b Equimolar solution of CTAB and KBr ($C_D = C_S = 0.3$ M). Variations of the extinction angle χ and of the birefringence intensity Δn as a function of the shear rate $\dot{\gamma}$ for different values of the temperature: (■) 30 °C, (□) 32 °C, (●) 34 °C, (○) 36 °C, (▲) 38 °C

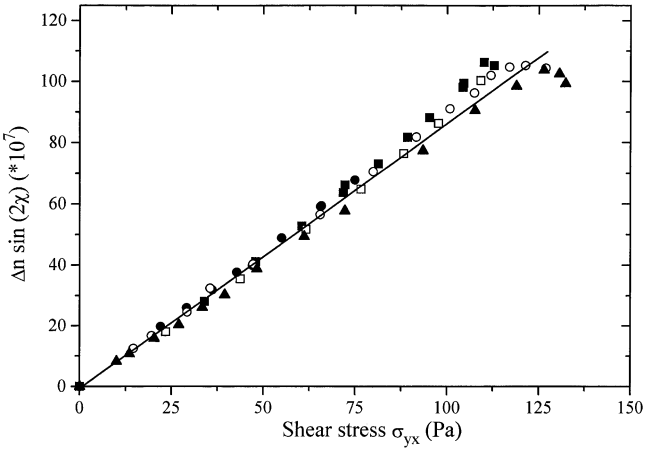

Fig. 3 Stress optical law $\Delta n \sin 2\chi = 2C\sigma_{yx}$ for the equimolar solution taken at different temperatures: (■) 30 °C, (□) 32 °C, (●) 34 °C, (○) 36 °C, (▲) 38 °C

Table 1 Stress optical coefficient C at different temperatures for the solution CTAB/KBr 0.3/0.3 M

Temperature [°C]	30	32	34	36	38
$C \times 10^7$ [Pa^{-1}]	0.46	0.44	0.45	0.45	0.41

Δn should reach a saturation value. This value is never found with this particular solution since a phase transition is triggered when $\dot{\gamma}$ reaches a critical value [13, 14]. If $\dot{\gamma}$ is further increased after this value, χ and Δn show a plateau behavior typical of a shear banding structure [15–17].

However, the range of shear rates corresponding to the first part of the curves is wide enough to test the validity of the stress optical law and this is shown in Fig. 3 where $\Delta n \sin(2\chi)$ is plotted against σ_{yx}. For each value of the temperature T, the points distribute well on each side of a straight line the slope of which is $2C$. The range of values of the shear stress σ_{yx} corresponds for each value of the temperature T to shear rates $\dot{\gamma}$ of the first part of the curves $\chi(\dot{\gamma})$. When σ_{yx} exceeds roughly 100 Pa, some discrepancies between the experimental points and the straight line start to appear, especially in the points corresponding to the lowest temperature. This behavior can easily be understood when we know that the shear rate approaches the critical value at which the shear banding flow occurs. In that case the stress optical law is probably no longer valid.

Shikata and co-workers [3], with the developments found in the refs. [18–20], have proposed a theoretical expression of C which is found to be inversely proportional to the absolute temperature T. In our work, the relative variation of T is too small in order to consider the observed variation of C with T as significant. It turns out that the absolute value of the coefficient C is 0.44×10^{-7} Pa^{-1} (see Table 1 for the values of C corresponding to the different temperatures) for this solution. This value is not in agreement with Shikata [3] or Wheeler [21] who proposed, respectively, 3.49×10^{-7} Pa^{-1} and 3.1×10^{-7} Pa^{-1} for a CTAB/NaSal solution at the concentration $C_D = 0.03$ M, $C_S = 0.23$ M. This result emphasizes that the concentration in surfactant, the nature and concentration in salt play an important part in the rheo-optical properties of these micellar solutions as we shall see in the following sections.

Set II: Constant surfactant concentration ($C_D = 0.3$ M) but increasing salinity

The second set of curves (Figs. 4a, b and 5) show the variation of χ and Δn (Δn in a log–log plot) versus $\dot{\gamma}$ and $\Delta n \sin(2\chi)$ versus σ_{yx} for four solutions in which C_D is kept constant while the molar concentration in salt $C_S = 0.1, 0.2, 0.3$ and 0.4 M. The temperature is kept constant at 30 °C. The increase of the concentration in salt results in an increase of the average length of the particles which thus orientated more easily in the flow.

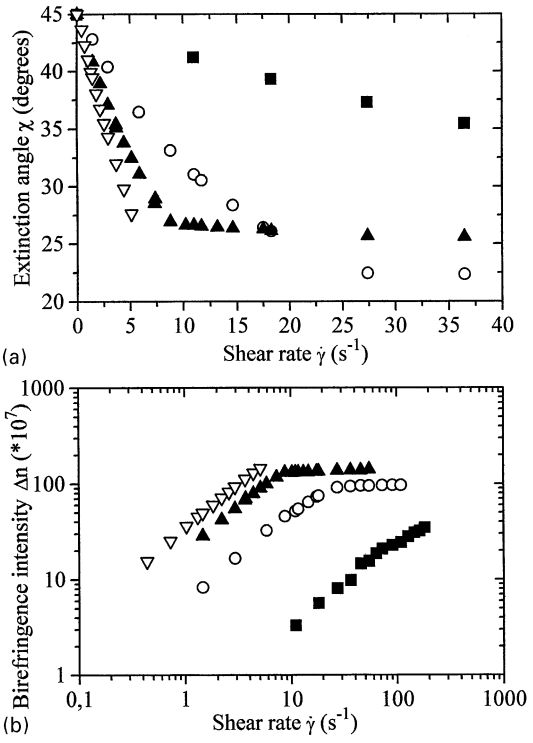

Fig. 4a, b The extinction angle χ and the birefringence intensity Δn (Δn in a log–log scale) as a function of the shear rate $\dot{\gamma}$ for four solutions (set II) of equal concentration in CTAB ($C_D = 0.3$ M) but in a solvent of increasing salinity C_S: (■) 0.1 M, (○) 0.2 M, (▲) 0.3 M, (▽) 0.4 M. The temperature is kept constant at 30 °C

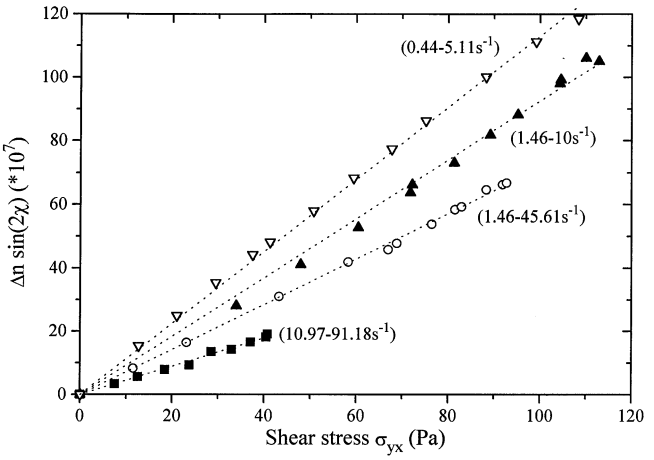

Fig. 5 Stress optical law $\Delta n \sin 2\chi = 2C\sigma_{yx}$ for the four solutions of set II (with $C_D = 0.3$ M and C_S: (■) 0.1 M, (○) 0.2 M, (▲) 0.3 M, (▽) 0.4 M) taken the same temperature 30 °C. The figures in brackets represent the corresponding range of shear rates $\dot{\gamma}$

This assumption is based on the fact that the viscosity of the solution increases when C_S is increased from 0.1 to 0.4 M. In consequence χ decreases more rapidly while the birefringence intensity Δn increases faster with $\dot{\gamma}$. In particular, for the less concentrated solution ($C_S = 0.1$ M black squares) the variation of χ over the entire range of $\dot{\gamma}$ is only a few degrees showing the difficulty for the small particles to align in a preferential direction. This solution containing small particles behaves nearly as a Newtonian fluid ($\chi \approx 45°$) in the region of small shear rates.

Figure 5 shows the curves $\Delta n \sin(2\chi)$ versus σ_{yx}. It can be seen that the stress optical law holds over a wide range of the shear stress. For each curve in Fig. 5 the corresponding range of shear rates is shown in brackets. The slope of each straight line is twice the optical coefficient C which varies significantly between 0.25 and 0.62×10^{-7} Pa^{-1} (the results are gathered in Table 2), the highest value corresponding to the solution with highest concentration in KBr.

Set III: Constant ionic force ($C_S = 0.1$ M) and increasing surfactant concentration

Finally, the third set of curves (Figs. 6a, b and 7) show the data obtained with four solutions of equal salinity, constant ionic force ($C_S = 0.1$ M), but with $C_D = 0.3, 0.4, 0.5$ and 0.6 M. With $C_S = 0.1$ M, the concentration in surfactant of 0.6 M is about the highest value we can use without the solution forming a liquid crystal even under the lowest value of $\dot{\gamma}$. The main results appear in Fig. 7 where $\Delta n \sin(2\chi)$ is plotted against σ_{yx}. Again the different experimental points are on average placed on each side of a straight line, the slope of which gives $2C$, and so the stress optical coefficient is found to vary between 0.25 and 0.96×10^{-7} Pa^{-1} (Table 2). The curve (full black squares) corresponding to $C_D = 0.3$ M has the lowest viscosity of the four solutions; thus, although the highest value of the shear rate is 91 s^{-1}, the corresponding value of the shear stress is only about 40 Pa. (The shear rate has been limited to $\simeq 90\,s^{-1}$ with this solution to prevent the formation of bubbles in the solution.)

Table 2 Stress optical coefficient C for different concentrations of salt and surfactant for a same temperature (30 °C)

CTAB/KBr[M]	0.3/0.1	0.3/0.2	0.3/0.3	0.3/0.4	0.4/0.1	0.5/0.1	0.6/0.1
$C \times 10^7$[Pa^{-1}]	0.25	0.36	0.46	0.62	0.42	0.75	0.96

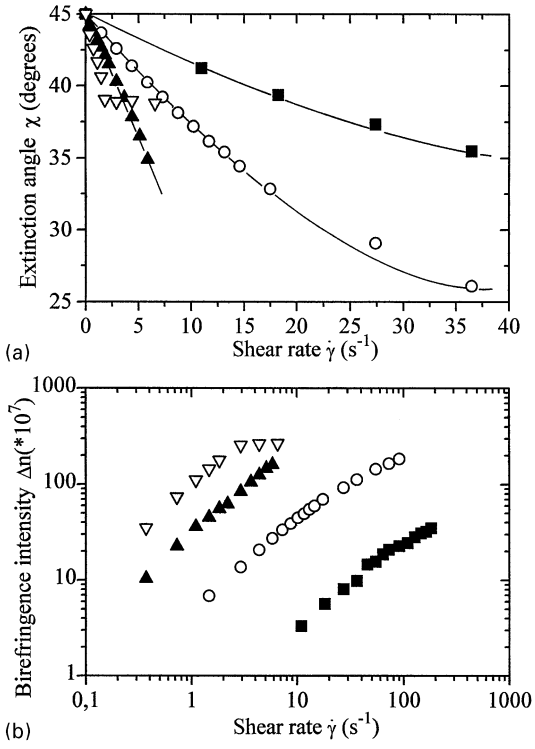

Fig. 6a, b The extinction angle χ and the birefringence intensity Δn (Δn in a log–log scale) as a function of the shear rate $\dot{\gamma}$ for four solutions (set III) of equal concentration in KBr ($C_S = 0.1$ M) but increasing concentration of CTAB C_D: (■) 0.3 M, (○) 0.4 M, (▲) 0.5 M, (▽) 0.6 M

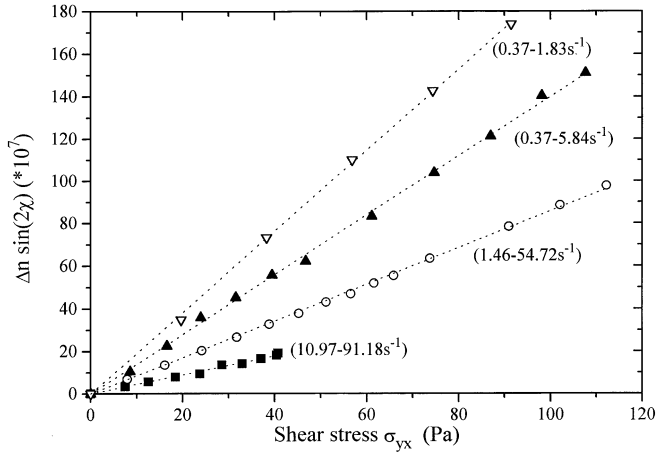

Fig. 7 Stress optical law $\Delta n \sin 2\chi = 2C\sigma_{yx}$ for the four solutions of set III (with $C_S = 0.1$ M and C_D: (■) 0.3 M, (○) 0.4 M, (▲) 0.5 M, (▽) 0.6 M) taken the same temperature 30 °C. The values in brackets represent the corresponding range of shear rates $\dot{\gamma}$

Although the order of magnitude of C is the same in all these results, the variation of the stress optical coefficient for each set of the experiments is nevertheless significant of a dependence of C on the physical characteristics of the different micellar solutions. This point shall be discussed later on in this paper.

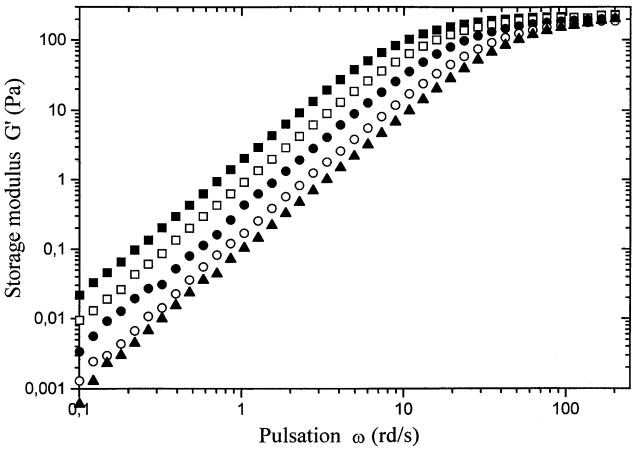

Fig. 8 G' versus ω for the equimolar solution ($C_D = C_S = 0.3$ M) at different temperatures: (■) 30 °C, (□) 32 °C, (●) 34 °C, (○) 36 °C, (▲) 38 °C

Rheological results

The same solutions are subjected to an oscillating shear stress in a cone–plane device to record the behavior of the storage modulus G' versus the angular frequency ω. The temperature is the same for all solutions and kept constant at 30 °C except for the equimolar solution.

The qualitative behavior of G' and G'' is the same for all the solutions and rather similar to the behavior of other surfactants solutions. In the range of small ω, G' is proportional to ω^2 as can be expected for a simple Maxwellian solution. Figure 8 is just one example of the behavior of G' with ω; all the curves $G'(\omega)$ behave at least qualitatively in the same way.

These values of G' are used to compute $G'(\omega)/\omega^2$, data which are then compared to the ratio $\Delta n \cos(2\chi)/2C\omega^2$ according to Eq. (4). Figures 9–11 represent (in log–log scale) the variations of these two quantities with $\dot{\gamma}$ or ω for the three sets of the results. The symbols represent the data computed from the birefringence measurements while the solid lines represent the variation of $G'(\omega)/\omega^2$ resulting from the dynamic measurements performed on the different solutions.

Figure 9 refers to the equimolar solution of CTAB/KBr (0.3 M), the data resulting from the birefringence measurements fit well on the different full curves corresponding to the different temperatures of $G'(\omega)/\omega^2$. The departure from the continuous curves decreases with the temperature and for $T = 38$ °C, the agreement is surprisingly good over a wide range of shear rates.

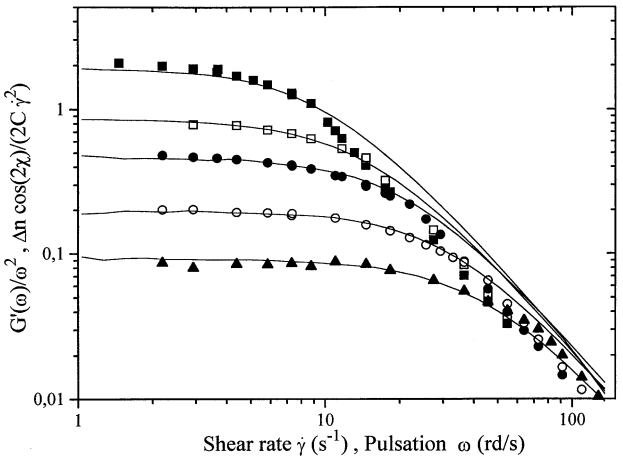

Fig. 9 The behavior of $G'(\omega)/\omega^2$ (in full line) and $\Delta n\cos(2\chi)/2C\dot{\gamma}^2$ (symbols) for the equimolar solution at five different temperatures: (■) 30 °C, (□) 32 °C, (●) 34 °C, (○) 36 °C, (▲) 38 °C

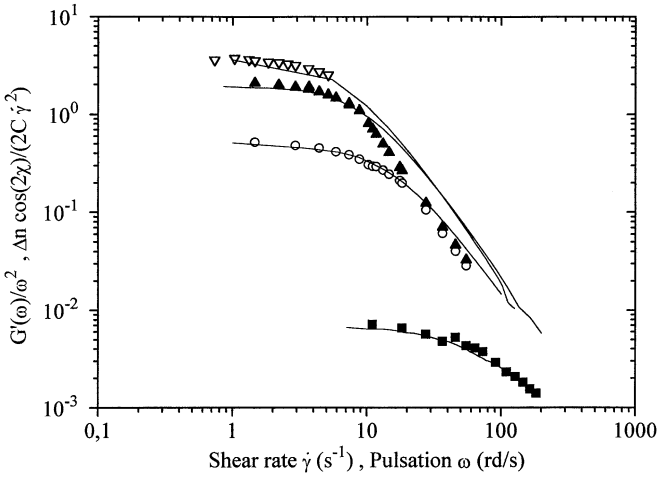

Fig. 10 Laun's law in the case of the four solutions of equal concentration in CTAB (set II) but increasing C_S: (■) 0.1 M, (○) 0.2 M, (▲) 0.3 M (▽) 0.4 M. The full lines come from dynamical measurements and the symbols are the results of the optical measurements

In Fig. 10 we have drawn $G'(\omega)/\omega^2$ for the second set (set II) of solutions. For each curve, in the range of low $\dot{\gamma}$ (or ω) $G'(\omega)/\omega^2$ exhibits a plateau behavior and then decreases. The symbols representing the computed values, $\Delta n\cos(2\chi)/2C\omega^2$ again fit quite well with the solid curves specially in the plateau region as expected from the theoretical relation (4) valid only in the limit of small ω or $\dot{\gamma}$. The same conclusions can be drawn from the results which appear in Fig. 11 (also in a log–log representation) concerning solutions of constant salinity and increasing surfactant concentration. The range of shear rates values over which we can say that Eq. (4) is satisfied widens with the concentration C_S when C_D is kept constant or with C_D when the salinity is constant.

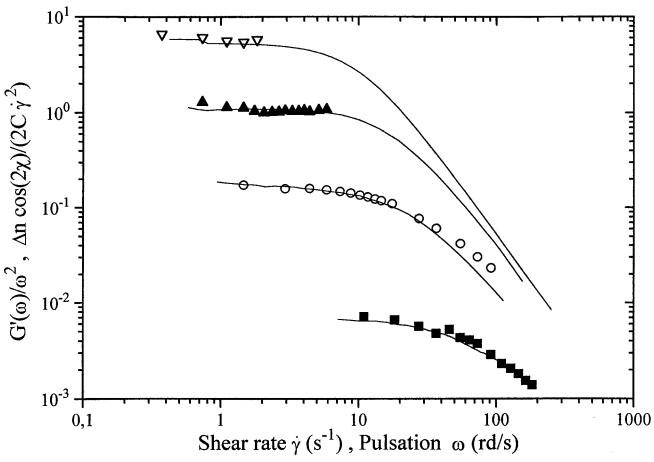

Fig. 11 Laun's law in the case of the four solutions of equal salinity (set III) but increasing concentration of CTAB C_D: (■) 0.3 M, (○) 0.4 M, (▲) 0.5 M (▽) 0.6 M. The full lines come from dynamical measurements and the symbols are the results of the optical measure ments

These results show that the first normal stress difference N_1 computed from the birefringence measurements using the stress optical coefficient C agrees well with the values of N_1 obtained from dynamical measurements of G'.

Discussion of the results

The stress optical law is found to be valid with a fairly good approximation for a wide range of shear stresses for the three sets of experiments. The main result is that the coefficient C computed from Eq. (1) for the different solutions is not a constant but depends on the concentration C_D of the surfactant and on the salinity of the solvent.

A simple theoretical expression for C, based on the Kuhn and Grün model [22] can be found in the book written by Fuller [23]. In this model, the micelle is assumed to behave like a flexible chain made of N_k freely jointed segments. Each segment, a Kuhn segment, is considered as a rigid elongated ellipsoid of revolution the anisotropy of polarizability of which is $\Delta\alpha = \alpha_1 - \alpha_2$ (1 and 2 refer, respectively, to a direction parallel and perpendicular to the backbone of the particle).

It turns out that

$$C = \frac{2\pi(n^2 + 2)^2\Delta\alpha}{45nk_BT}, \tag{5}$$

where the following terms n and k_B are, respectively, the average refractive index and Boltzman's constant.

It is readily seen from Eq. (5) that C should decrease when the absolute temperature increases. However the dependence of C on the temperature is not made

evident: no significant variation is found probably because of the limited range of temperature investigated. The solution CTAB/KBr is not an ideal mixture to test this dependence since it precipitates when the temperature falls under 30 °C and becomes weakly birefringent above 38 °C. Assuming that $\Delta\alpha$ is itself independent of T, the expected variation of the coefficient C with T computed from Eq. (5) should be a decrease of a few percent ($\simeq 2.5\%$); we found a slight decrease of C but the variation, although of the same order of magnitude, is too small to confirm the law.

As already mentioned, the sign of the birefringence intensity Δn is negative for all the solutions. This result indicates that the main contribution to the birefringence of the solution is the intrinsic birefringence Δn_i of the micelles. The contribution of the form birefringence Δn_f is thus of little importance, as confirmed by the stress optical law which applies well in the different ranges of shear rates.

The polarizability of the whole solution results from the contribution of each micelles, not only by their individual intrinsic polarizability but also by their orientation under flow. This orientation is governed by a distribution function f and the polarizability of the whole medium is an average of the intrinsic polarizability by the distribution function f. Assuming that the Lorentz–Lorenz equation [24] is valid, the birefringence can then be calculated. It turns out that Δn, which is a quite complicated expression, will depend on the mean square of the end to end distance $\langle r^2 \rangle$ and be simply proportional to the polarizability $\Delta\alpha$ of a single Kuhn segment [25].

The intrinsic birefringence of a particle is defined as the difference between the principal indexes of refraction n_1 and n_2 of the particle (1 and 2 refer, respectively, to a direction parallel and perpendicular to the backbone of the micelle). If the birefringence Δn is negative then the polarizability anisotropy $\Delta\alpha$ is also negative and α_1 which is the polarizability in the direction of the longest dimension of the micelle is the smallest one.

Let us assume with Shikata that the micelles are formed by the stacking of disk-shaped monomers (see Fig. 12 taken from ref. [3]). In each monomer, the individual cations of surfactant are arranged in a kind of rosette with the Br^- ions and the water molecules in the vicinity of the head groups to ensure the cohesion of the structure.

When the concentration in salt is increased or, in a solution of constant salinity, when the amount of surfactant is increased, the micelles get longer but we can assume that the radius of the monomer is unchanged. It is thus reasonable to assume that the polarizability, α_2 remains unchanged in this direction but not in the direction of the backbone of the chain, since the length of a Kuhn segment must be affected when the average length of the particle is changed.

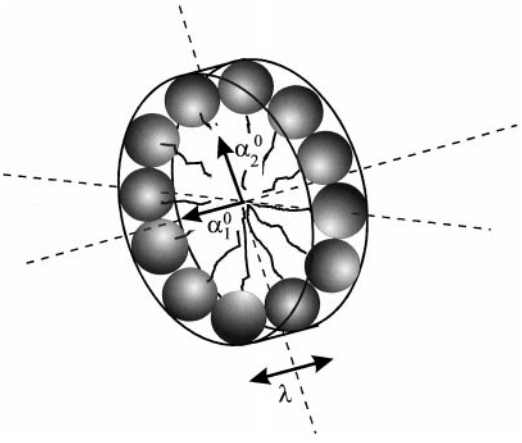

Fig. 12 Schematic representation of a monomer of a micelle as seen by Shikata et al.

Let $\Delta\alpha^0 = \alpha_1^0 - \alpha_2^0$ be the polarizability anisotropy of such a monomer, $\Delta\alpha$ is expressed as [3, 19]

$$\Delta\alpha = \frac{\Delta\alpha^0 \langle r^2 \rangle}{L\lambda} = \frac{2\Delta\alpha^0 q}{\lambda} \quad , \tag{6}$$

where λ is the thickness of a monomer and q the persistence length of the micelle. If the absolute value of $\Delta\alpha$ increases with C_S or C_D, this implies that the ratio $\langle r^2 \rangle / L$ increases too since $\Delta\alpha^0$ and λ remain constant. Equation (5) allows also for a simple calculation of $\Delta\alpha$ the polarizability of a Kuhn segment. Assuming $C = 0.44 \times 10^{-7}$, 1.33 for the mean refraction index of the solution and a temperature of 300 K, we get $\Delta\alpha = 1.2 \times 10^{-28}\,m^3$. This value is smaller than that found by Shikata ($8 \times 10^{-28}\,m^3$) but he studied the system CTAB/NaSal which is known to be different from the couple CTAB/KBr since the Sal^- ions behave like a co-surfactant.

Conclusion

In this work, we have shown that the stress optical law holds well in wide ranges of shear stresses for different solutions of CTAB/KBr forming entangled micellar solutions. The optical coefficient C computed from Eq. (1) allows for the determination of the first normal stresses difference N_1 with the help of Eq. (3).

Laun's rule (see Eq. (4)) allows then for the comparison of these two sets of values for N_1 which are found to be in very good agreement. It must be emphasized that two different techniques (permanent flow birefringence and dynamical rheological measurements) were used to calculate N_1 and this gives credit to the numerical values of C that we propose in this work.

C is found to decrease with the temperature as predicted by Eq. (5), but increase with either the concentration C_D of the surfactant or C_S of the salt. As far as optical experiments are concerned, CTAB has been mainly mixed with NaSal, thus we lack elements of comparison. Further experiments will be shortly performed with different system in order to study the behavior of the stress optical coefficient C, especially with different hydrocarbon chain lengths.

References

1. Scheraga HA, Backus JK (1951) J Am Chem Soc 73:5108–5112
2. Backus JK, Scheraga HA (1952) J Colloid 508–521
3. Shikata T, Dahman SJ, Pearson DS (1994) Langmuir 10:3470–3476
4. Wunderlich I, Hoffmann H, Rehage H (1987) Rheol Acta 26:532–542
5. Hofmann S, Rauscher A, Hoffmann H (1991) Phys Chem 95(2):153–164; Rehage H, Hoffmann H (1988) J Phys Chem 92:4712–4719
6. Janeschitz-Kriegl H, Papenhuijzen JMP (1971) Rheol Acta 10:461–466
7. Lodge AS (1956) Trans Faraday Soc 52: 120–130
8. Doi M, Edward SF (1978) J Chem Soc Faraday Trans 2 74:418–432
9. Janeschitz-Kriegl H (1987) Polymer Melt Rheology and Flow Birefringence. Springer, Berlin
10. Vinogradov GV, Malkin AYa (1977) Rheology of Polymers. Springer, Berlin
11. Laun HM (1986) J Rheol 30:459–501
12. Decruppe JP, Hocquart R, Wydro T, Cressely R (1989) J Phys France 50:3371–3394
13. Decruppe JP, Cressely R, Makhloufi R, Cappelaere E (1995) Colloid Polym Sci 273:346–351
14. Decruppe JP, Cappelaere E, Cressely R (1997) J Phys II France 7:257–270
15. Schmitt V, Lequeux F, Pousse A, Roux D (1994) Langmuir 10 3:24–35
16. Berret JF, Roux DC, Porte G, Lindner P (1994) Europhys Lett 25 7:521–526
17. Spenley NA, Cates ME, McLeish TCB (1993) Phys Rev Lett 71 6:939–942
18. Doi M, Edward SF (1986) The Theory of Polymer Dynamics. Oxford University Press, Oxford
19. Flory PJ (1969) Statistical Mechanics of Chain Molecules. Interscience Publishers, New York
20. Treloar LRG (1975) The Physics of Rubber Elasticity. Clarendon Press, Oxford
21. Wheeler EK, Izu P, Fuller GG (1996) Rheol Acta 35:139–149
22. Kuhn W, Grün F (1942) Kolloid-Z 28: 248–271
23. Fuller GG (1995) Optical Rheometry of Complex Fluid. Oxford University Press, Oxford
24. Lorentz HA (1880) Ann Phys Chem 9:641; Lorentz HA (1915) Theory of Electrons. 2nd ed. Dover reprint, New York; Lorenz L (1880) Ann Phys Chem 11:70
25. Jerrard HG (1959) Theory of streaming double refraction Chem Rev 59(3):400